

## 13R.3

# REAL-TIME COMPARISONS OF VPR-CORRECTED DAILY RAINFALL ESTIMATES WITH A GAUGE MESONET

Aldo Bellon\*, GyuWon Lee, Alamelu Kilambi and Isztar Zawadzki  
J. S. Marshall Radar Observatory, McGill University, Montreal, Canada

### 1. HISTORICAL BACKGROUND

From the very early years of operational radar meteorology at McGill, Marshall (1957), a basic product for a variety of applications has remained the CAPPI map, subsequently generated since the late 60's from the available 24 elevation angles every 5 minutes. On account of the fairly extensive ground clutter of our S-band radar which furthermore is located in the shallow valley of the St-Lawrence River with a high probability of anomalous propagation (AP), it was mandatory during those years of reflectivity-only data to centre the CAPPI at a fairly high altitude, namely at 10,000 ft (or ~3 km), Marshall and Ballantyne (1975). The advent of digital data by the mid 70's allowed for the interpolation over the known regions of normal ground clutter and thus permitted a lowering of the CAPPI to 2 km. Although the presence of the melting layer was well known, its impact was generally ignored or considered not to be important since most of the emphasis was then on the detection and forecasting of severe convective weather (as implied by our initial name of Stormy Weather Group). However, when precipitation estimates were routinely transmitted to the local forecast office in the mid 80's by the first version of our automatic radar processing system, flash floods warning were occasionally issued by the forecasters on the basis of accumulations generated from CAPPIs centered near the height of the bright band peak. A subsequent version of such system called RAPID (Radar data Analysis, Processing and Interactive Display) enabled the forecasters to at least properly recognized such gross overestimations of surface rainfall. It provided a range-dependent vertical profile of reflectivity (VPR) with every CAPPI and accumulation map, the VPR accompanying the latter being integrated over the appropriate time interval. Our first attempt at actually providing VPR corrected surface rainfall estimates was thus more readily achieved by correcting the 1-h accumulations, (Bellon and Kilambi 1999). The need to correct for the VPR had by then already been recognized by many researchers, Joss and Waldvogel (1990) Fabry et al. (1992) and Joss and Lee (1995) among others while Koistinen (1991) actually implemented an operational VPR correction of daily rainfall estimates. Techniques for enabling a correction on a shorter time scale were then devised by several investigators, (Andrieu and Creutin 1995; Kitchen 1997; Smyth and Illingworth 1998). The

various algorithms proposed, whether based on a mean or locally identified VPR, were eventually verified with one or several days of surface "ground truth" as provided by raingages, (Vignal et al. 1999; Vignal et al. 2000; Seo et al. 2000; Dinku et al. 2002; Germann and Joss 2002). The largest sample evaluation has been carried out by Vignal and Krajewski (2001) using two years of WSR-88D data and the corresponding rain gauge observations from the Oklahoma Mesonet. It is recognized that the results of such comparisons are not only dependent on the skill of the various VPR correction algorithms, that is, on their ability to take into account the actual space-time variability of the VPR, but also on the relative importance of the other well known sources of radar-gauge differences, namely, radar calibration, and possible rain-path and wet radome attenuation (for C-band), residual ground clutter and/or removal of precipitation by such procedure, radar-gauge temporal and spatial sampling differences and the variability of the drop size distribution that affects the conversion of radar reflectivity into a rainfall rate. A simulation study by Bellon et al. (2005) has attempted to isolate the expected improvement of a basic VPR correction technique due solely to the VPR as a function of bright band height, accumulation interval, averaging area and uncertainties in the bright band height. By allowing for a realistic variability of the VPR, it was found that the latter limits the possible improvement by an amount greater than expected. Since the reviewers of that paper urged us to also evaluate our technique with actual surface measurements, the recent installation of a Mesonet during the summer of 2004 has permitted us to implement such a task in real-time. In this paper we thus report on all the comparisons of daily rainfall estimates continuously made from April to June 2005 that were archived in real-time as well as on the results from the regeneration of radar accumulations maps during the significant stratiform events from fall 2004 (September to end of November).

### 2. VPR CORRECTION METHODS WITH THE MCGILL RADAR

During approximately the past eight years, as part of the McGill RAPID system, we have been constantly developing and updating various VPR correction schemes for the real-time surface radar rainfall estimates provided to the Montreal Weather Office. These maps are in the form of (240 x 240) arrays at both 1- and 2-km resolution, thus extending to 120 and 240 km from the radar respectively. Currently, at every hour, four types of 1-h accumulations are generated by RAPID.

---

\*Corresponding author address: Aldo Bellon, J. S. Marshall Radar Observatory, P. O. Box 198, Macdonald Campus, Ste-Anne-de-Bellevue, QC, Canada.  
H9X 3V9 E-mail: [aldo.bellon@mcgill.ca](mailto:aldo.bellon@mcgill.ca)

a) VPR uncorrected ( $C_0$ )

Even though we refer to these estimates as “uncorrected” from the VPR point of view, their generation requires considerable processing of the raw data of the 24 elevation angles which are recorded at a resolution of  $1^\circ$  and of 1 km up to 120 km, (and of 2 km between 120 and 240 km). This data set that is actually collected at a PRF of 600 or of 1200 Hz depending on the elevation angle is first corrected for range and velocity folding. Then, due to the absence of a zero-velocity notch filter at the signal processing level, pixels with normal and AP ground clutter are first identified at this resolution by means of an algorithm that computes the standard deviation of reflectivity from the seven 150-m gates before they are averaged into a 1-km bin. The 1 km by  $1^\circ$  pixel is then declared ground echo if it exceeds a threshold (3.3 dB) and if the absolute value of the mean radial velocity over the 1-km distance is below 1.5 m/s. Precipitation information over these ground echo pixels is obtained by a range-azimuth interpolation of the neighboring ‘raining’ pixels. However, ground echoes are simply removed and no interpolation is performed over ‘near zero-velocity’ pixels if the ratio of the ground echo area with the precipitation area exceeds another threshold. A technique similarly based on the characteristics of radar echoes proposed by Lee et al. (2005) is also being considered for our data. After the polar to Cartesian transformation onto 1- and 2-km resolution grid areas at a user-selectable “pseudo-CAPPI” height (now usually set at 1.5 km), the resultant maps available every 5 minutes are integrated over a desired time interval (typically 1-h) using an advection procedure that takes into account the propagation velocity of the precipitation area. This is done in order to avoid quantization effects caused by the difference

in the time and space scales of the data set. Longer accumulations are simply obtained by summing the pre-generated 1-h accumulations.

b) Correction of 1-h accumulations ( $C_1$ )

Fig. 1a exemplifies the overestimation of an uncorrected 1-h accumulation map ( $C_0$ ) generated from CAPPIs centered at 2 km, the height of the bright band peak. The azimuthally-averaged and time-integrated (1-h) range-dependent VPR shown on the bottom right-hand corner of the display would immediately warn the user of the unsuitability of such an estimate in representing surface precipitation. The integration is performed in reflectivity (Z) units. This VPR also exemplifies the widening vertical influence but with diminishing intensity of the bright band with range as sampled by a scanning radar with approximately a  $1^\circ$  beam width. Five VPRs are in fact derived over 20-km range intervals from 10 to 110 km and at a vertical resolution of 0.2 km. Such a narrow vertical resolution may be appropriate for the lower altitudes because each 0.2 km slice is sufficiently sampled by the near-horizontal lower elevation angles, but is unsuitable for higher altitudes where fewer data points from a drastically reduced number of less horizontal elevation angles can fall inside the upper slices. On the other hand, a large proportion of the data at the lower altitudes obtained by interpolation over the identified ground echoes, as described in 2a above, are thus not actually used in the derivation of the space-time VPR. A logarithmic vertical spacing would still have been more desirable, but the integration over a sufficiently large space-time domain avoids the shortcomings of a constant height resolution.

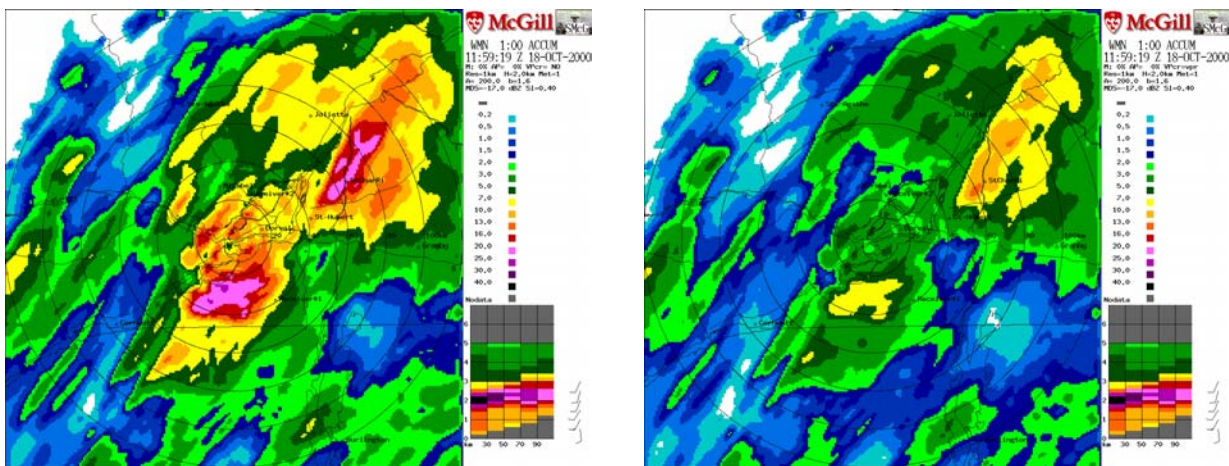


**Fig. 1:** Example of a  $C_1$  correction (right panel) of a 1-h accumulation map made from CAPPIs centered at the height of the bright band peak, ( $C_0$  in the left panel). Maps are at a resolution of 1 km with range rings 20 km apart up to 120 km. This and similar figures are best viewed with a magnification of at least 150%.

Our preliminary efforts, detailed in Bellon and Kilambi (1999), consisted in correcting the 1-h accumulation on the basis of the reflectivity difference

between the 2-km height and a suitably lower reference height. The lowest height is seen to be a function of range but it is preferable to select the

reference height to be at least 0.2 km above the minimum height in order to avoid any possible contamination by residual ground echoes. (Note that even though the VPR shown seems to indicate that our accumulation maps should be based on low angle PPIs rather than on 1.5 km CAPPPIs, the VPR at the low heights, as just stated, is based on the relatively few pixels with significant radial velocity located at the ground echo-free regions). The five correction factors in dBZ units obtained for each of the computed VPRs are converted into rainfall rate factors and interpolated in range at every kilometer. This technique presupposes that the reference height is not affected by the lower portion of the bright band. In order to reduce this possibility, we have opted to use only the first four VPRs, and extend the correction obtained for the 4<sup>th</sup> VPR in the 70-90 km interval up to the 120-km range. The corrected accumulation shown in Fig 1b reveals that this simple approach is at least qualitatively suitable for purely stratiform situations since the rainfall amounts are considerably reduced as intended. If it is known that the reference height is indeed contaminated by the melting layer, the reference reflectivity is taken at a height of the bright band top. The recognition of this problem is aided by the information about the 0°C height from model output. We use the Rapid Update Cycle (RUC) forecasts: [//maps.fsl.noaa.gov/](http://maps.fsl.noaa.gov/) but it can also be deduced from the height of the peak reflectivity when the profile has been identified as that of a bright band. The bright band top can then be determined from the observed VPR as where the 2<sup>nd</sup> derivative or curvature in the reflectivity drop above the bright band peak exceeds a threshold ( $\sim 0.8 \text{ dBZ}/200\text{m} / 200\text{m}$ ), or where a large drop in reflectivity across a 200 m layer in that region is followed by a much smaller drop over the next two layers. Otherwise the bright band top is assumed to be a function of the peak reflectivity and range. When no bright band has been identified, it is assumed to be half a beam width above the height of the 0° C isotherm as provided by the RUC model.

Because the 2-km resolution maps extend up to a range of 240 km, it is desirable to estimate the appearance of the 4<sup>th</sup> VPR at successive ranges up to 240 km using a Gaussian simulation technique outlined in the appendix of Bellon et al. (2005) and illustrated in Fig. 3 of that paper. The proper correction factor for a given far range is thus obtained from the difference between the reflectivity of the Gaussian simulated profile at the true height of that range and the reflectivity at the reference height on the observed 4<sup>th</sup> VPR.

### c) Optimum Surface Precipitation (OSP or C<sub>2</sub>)

While method C<sub>1</sub> is relatively simple, being readily applicable for Cartesian accumulation maps already generated at historically higher altitudes ( $\sim 2$  km), it has the disadvantage that all rainfall amounts are corrected using their corresponding single VPR, regardless of whether the rain fell at the beginning or at the end of the accumulation interval. Moreover, after completing

the accumulation process, useful information regarding the stratiform or convective nature of the precipitation is lost. It is well known that a VPR correction should be applied to only the stratiform portion of a precipitation system, something that cannot be achieved with the "one-shot" approach of method C<sub>1</sub>. Therefore, an optimum surface precipitation (OSP) algorithm, referred here as method C<sub>2</sub>, has been devised that seeks to correct every polar pixel of each of the 12 "pseudo-CAPPPIs" needed for a 1-h accumulation. On account of the improved ground echo identification, removal and subsequent interpolation technique, we can afford to lower the altitude for the "pseudo-CAPPPI" maps to 1.3 or 1.1 km. Such heights are strictly true up to a distance of  $\sim 90$  km, sloping up to 2 km at a range of 125 km according to the 1<sup>st</sup> elevation angle of 0.5 degrees. The 2<sup>nd</sup> elevation angle at 0.6 degrees and 600 PRF is then used for farther ranges, (the 1<sup>st</sup> angle being at 1200 PRF).

At every radar cycle, a VPR with similar spatial characteristics as in Fig. 1a is derived but integrated over a user-selectable shorter time interval than one hour (typically 30 or 45 minutes). Unlike the method proposed by Germann and Joss (2002), the data from the required 5-min volume scans inside this interval are equally weighted. Convective pixels, identified according to a procedure described later, are excluded in the derivation of the space-time averaged VPR. The stratiform pixels of the "pseudo-CAPPPI" are corrected in a fashion as described for method C<sub>1</sub>. In order to avoid improper corrections based on insufficient data, the VPR must have a vertical extent of at least 2 km. We provide in Fig 2 an example of a C<sub>2</sub> correction where a higher CAPPPI height is used to better accentuate the results of a VPR correction. Since the uncorrected CAPPPI map at a height of 2 km is just below the bright band, the reduction of the reflectivities at shorter range is mainly due to the lower height of 1.1 km, but the reduction at medium ranges ( $\sim 120$  to  $\sim 160$  km) is due to the bright band correction. At farther ranges, the reflectivities taken in the snow are then increased as can be plainly seen on the corrected map, especially for ranges beyond 180 km. When attempting to extend the VPR correction to such far ranges, it is very crucial to apply this positive correction to only the stratiform portions of a precipitation system, that is, snow, otherwise huge overestimations would result from embedded convection that requires little or no correction. Conversely, the inability to recognize a reflectivity as convective at closer range at a height within the bright band influence would cause an underestimation of the precipitation.

We identify convective pixels according to a criteria suggested by Smyth and Illingworth (1998) which we slightly modified to a reflectivity of 32 dBZ 2 km above the bright band peak. In order to ensure that no convective pixels are missed, an upper level VIL (Vertical Integrated Liquid), or UVIL map (Greene and Clark, 1972) is generated by integrating  $Z^{4/7}$  from a height of 4 km. A pixel that may have gone undetected

according to the previous test is declared as such if the UVIL value exceeds a threshold of 1 kg/m<sup>2</sup>. Convective pixels are not modified (although we envisage a possible increase of ~2 dBZ/km for their correction at heights above ~3 km), but the C<sub>2</sub>

technique allows for a different Z-R relationship for the stratiform (Z=200R<sup>1.5</sup>) and convective pixels (Z=300R<sup>1.4</sup>). The former is based on the analysis of 5 years of disdrometric data in the Montreal region by Lee and Zawadzki (2005a).

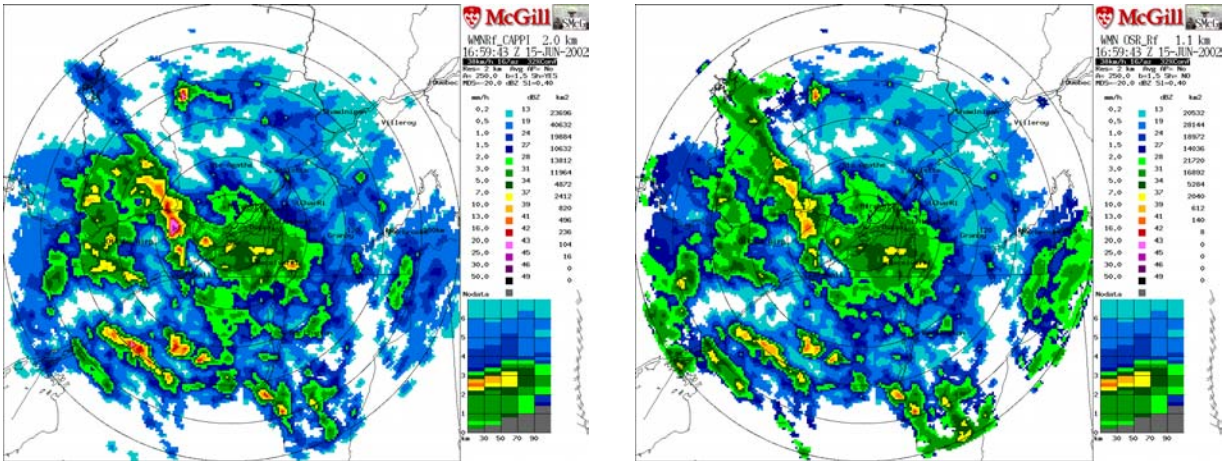


**Fig. 2:** Example of an uncorrected 2-km CAPPI map and a 1.1-km “pseudo-CAPPI” map (or OSP map) corrected according to the method described in section 2c. Maps are at a resolution of 2 km with range rings 40 km apart up to 240 km.

During the time of Fig. 2 at ~1700 UTC, the entire precipitation is stratiform. However, between 2200 and 2300 UTC, a convective cell developed within the stratiform precipitation. As illustrated in Fig 3, the C<sub>1</sub> correction properly reduces the near range overestimation due to the bright band but erroneously also reduces the convective rainfall seen just beyond 160 km. The C<sub>2</sub> method recognizes this precipitation as convective and thus maintains most of the associated higher rainfall estimates. We admit that the results shown later, being based on comparison with gauges at relatively close distances from the radar, (< 120 km), cannot ascertain to what extent this particular aspect of our procedure is successful at longer ranges. A delicate balance needs to be achieved between the urgency to reduce the excessive estimates of rainfall from bright band reflectivities and the necessity to maintain the strong rainfalls from convective cells at all ranges. In our ongoing modification of the algorithm, the limitation of any positive correction to only reflectivities below a certain threshold (and thus likely snow), appears to be a way to ensure both goals.

The recognition of a low bright band affecting the reference range is used with C<sub>2</sub> in a manner similar to that of C<sub>1</sub> as is the procedure for estimating the correction for ranges beyond the 4<sup>th</sup> VPR. The uncertainty associated with estimating the bright band top renders the subsequent estimates of surface rainfall that used it as the reference more prone to errors as well as to a greater time and space variability of such errors. Two additional refinements have been incorporated with C<sub>2</sub>. It can identify a VPR as low level

growth when a reflectivity maximum is observed near or at the reference height but far away from a higher 0° C isotherm height. The latter information is needed so as not to misinterpret the top portion of a very low bright band as low level growth. In addition to the correction determined from the VPR, the identification of low level growth permits an extra increase of up to 3 dBZ, (depending on the observed vertical gradient just above the reference height) in order to account for the reflectivity growth between the reference height and the actual surface. An attempt has also been made to identify evaporation when weak reflectivity aloft is observed with no reflectivity in the lowest two layers of the VPR. In this situation, the reflectivity at the “pseudo-CAPPI” height is decreased by as much as 5 dBZ if it is less than 20 dBZ. From our experience, evaporation can be detected during the approaching phase of an extensive low pressure system, particularly in winter, with echoes clearly only aloft. It is not as successful with scattered, small scale cells in the dry air mass in the departing phase of a frontal system, mainly because the observed VPR is of insufficient depth to risk a correction. Therefore, we must state that the skill of these two refinements to the C<sub>2</sub> technique cannot be properly assessed by our experiment since we expect their importance to be relatively minor in our regions. Finally, the C<sub>2</sub> method provides one obvious improvement in the north-west quadrant beyond 90 km which is severely affected by beam blocking of lower elevation angles by nearby hills. This is simply achieved by selecting higher unblocked elevation angles in the generation of the OSP CAPPI map for the sector so affected between

300 and 330 degrees azimuth. In so doing, the measurements are more likely to be influenced by the bright band but the subsequent correction readily compensates for it. The higher elevations, however, do diminish the maximum useful range of such corrections.

We point out that we have applied both the  $C_1$  and  $C_2$  algorithms with some success in purely snowfall situations, generally yielding higher amounts than what

would have been observed on the uncorrected “pseudo-CAPPI” height. However, before attempting a quantitative evaluation, a more robust algorithm that combines the derived VPR with the observed or model forecast vertical temperature structure is needed in order to infer hydrometeors type and size and thus be able to more truly correlate the reflectivity aloft with surface snowfall rates.

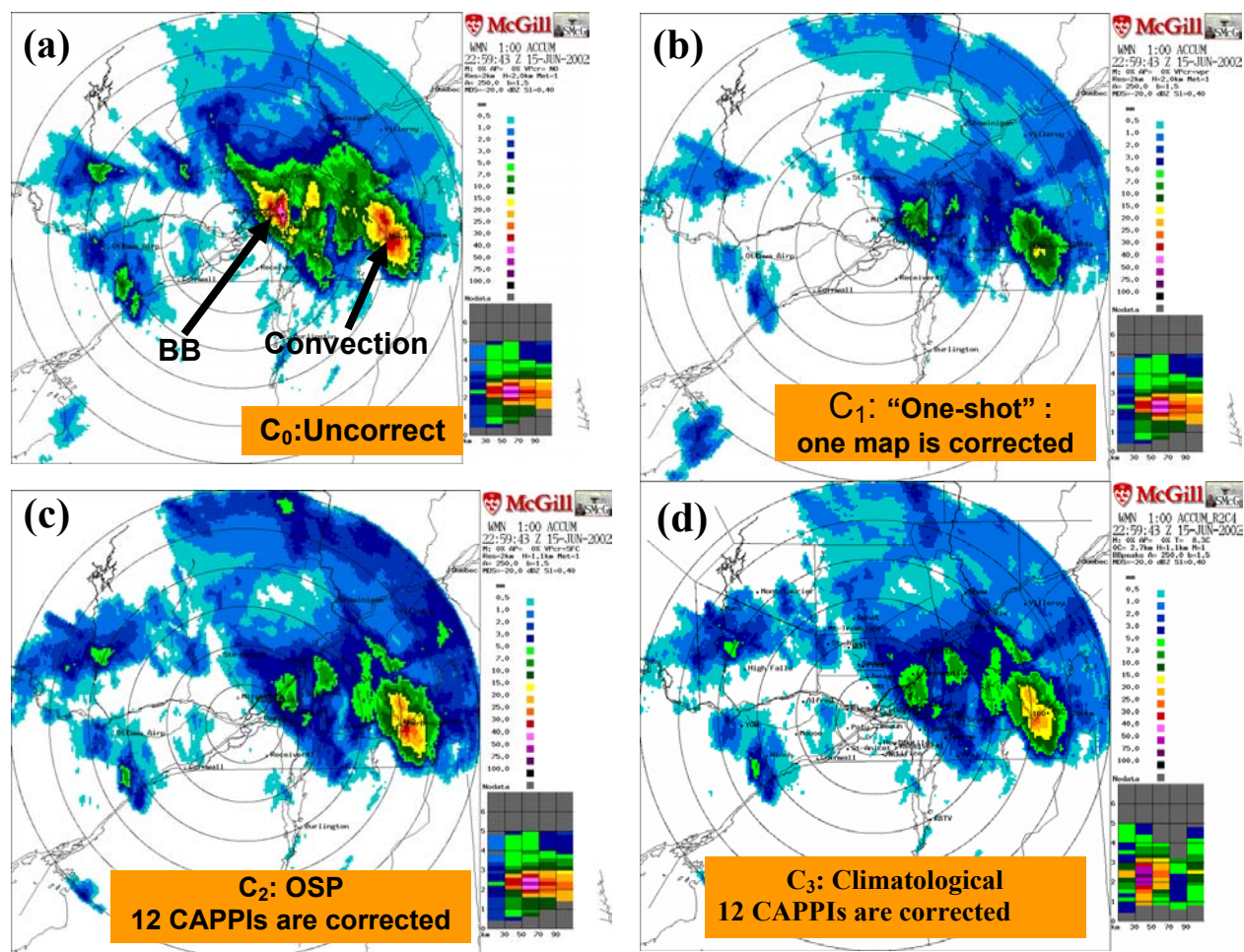


**Fig. 3:** Uncorrected and  $C_1$ ,  $C_2$  and  $C_3$  corrected 1-h accumulations showing the importance of recognizing convective pixels in a proper VPR correction scheme. Maps are at a resolution of 2 km with range rings 40 km apart up to 240 km.

*d) Climatological Correction ( $C_3$ )*

The three procedures described so far need a sufficient amount of precipitation echoes within 90 km in order to derive a VPR from which reliable correction factors can be derived. An averaged space-time reflectivity is thus required to be available over at least 10 slices (2 km), otherwise information from one of the VPRs computed for the other range intervals is used. When none are available, a correction cannot be attempted. In order to circumvent this problem and to

evaluate a technique that is not dependent on the variability of observed VPRs, correction factors computed on the basis of a climatological VPR can be used. In our recent work, Bellon et al. (2005), we have used a data set of 287 hours of extensive stratiform precipitation in order to compute climatological profiles that are also a function of the surface reflectivity. This stratification is intended to improve correction factors, which are at least partly dependent on precipitation intensity, a fact that is not taken into account with the observed VPRs where all reflectivities are combined in

the averaging process. Our simulation also permitted us to deduce their appearance at various ranges while still considering as ground truth the surface reflectivity at near range. These profiles are repeated here as Fig. 4. If the height of the 0°C isotherm is known from the RUC model, a correction factor can be determined from an observed reflectivity at any range as described by Eq. (2) of that paper. Mittermaier and Illingworth (2003) as well as our own simulations (Bellon et al. 2005) point out the magnitude of errors resulting from an inaccurate height. We must also be aware of the relatively large standard deviation of these climatological curves, particularly in the snow region where it is of the order of about 5-8 dBZ. Also note the narrow range of possible reflectivity at heights of more than 2 km above the bright band peak, compared with the broader spectrum of reflectivities at the bright band

peak as well as at the surface. This implies that a small error in selecting the most suitable curve in the snow would entail a significant error in the determination of the surface reflectivity. This problem was correctly recognized by Fabry et al. (1992). Seo et al. (2000) also commented that correction factors obtained inside the bright band are likely to yield better estimates of the surface rainfall than correcting measurements taken in the snow region. Considering these difficulties, we just intend here to evaluate the skill of this climatological algorithm mainly in relation to  $C_0$  for possible implementation during the incoming phase of a precipitation system. The sparseness of the radar network in Canada is such that we cannot rely on the overlapping coverage of a nearby radar for better surface rainfall estimates at medium and long ranges.

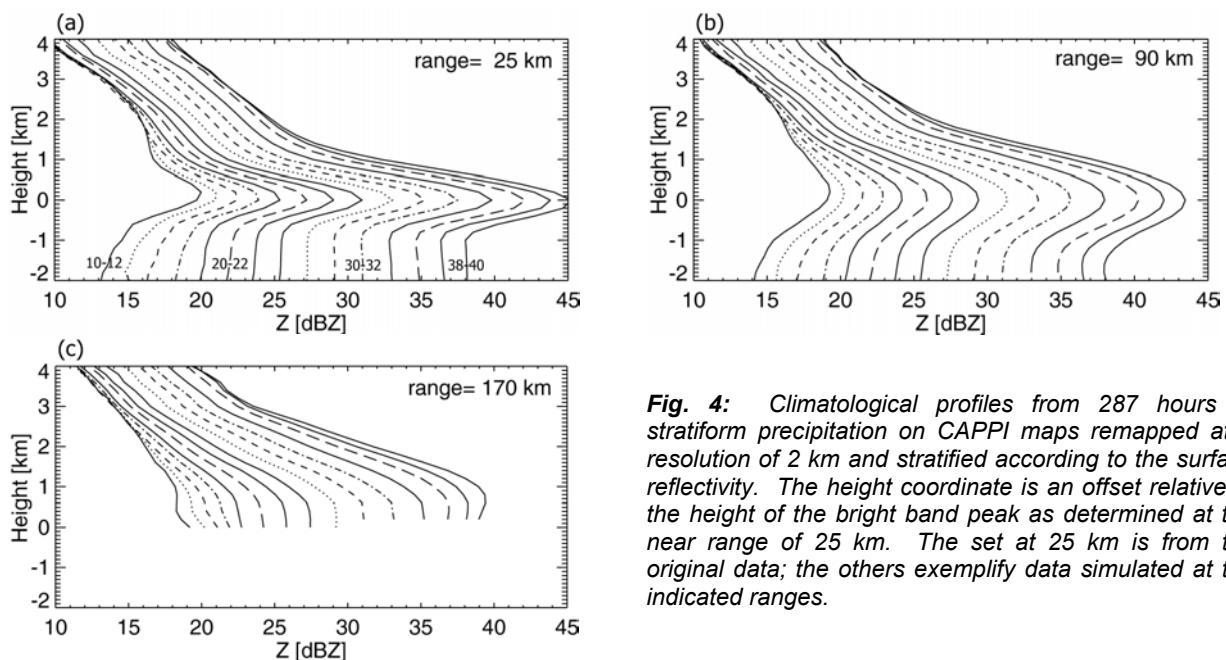


**Fig. 4:** Climatological profiles from 287 hours of stratiform precipitation on CAPPI maps remapped at a resolution of 2 km and stratified according to the surface reflectivity. The height coordinate is an offset relative to the height of the bright band peak as determined at the near range of 25 km. The set at 25 km is from the original data; the others exemplify data simulated at the indicated ranges.

### 3. EXPERIMENTAL SETUP

The McGill RAPID system provides maps of various radar-related parameters as specified on a menu by the user. In particular, accumulation maps over any time interval can be requested at a flexible frequency, but it is customary to generate 1-h accumulations every 5 minutes, and longer accumulations, (6-, 12- and 24-h) at every hour. Each of these accumulations is in turn generated according to the four methods described in section 2. Until last year, these various options for the surface precipitation product were not verified except on the basis of some subjective visual assessment and acceptance by the forecasters on duty, (and by the algorithm developers). The installation beginning in the spring of 2004 of a Mesonet with gauges reporting rainfall measurements in real-time has finally provided the stimulus for comparing the relative skill of the VPR correction

methods used. Twenty to 25 gauges were operational by mid-summer until spring 2005 when the total was increased to ~40 as shown in Fig. 5. All except one in the WNW at 140 km are located inside the typical (240 x 240) 1-km resolution map centered over the McGill radar. Consequently, at most 5 or 6 could be considered at a sufficiently long range to evaluate the procedure for the Gaussian simulation of the farthest VPR and none are at ranges enabling a verification of the increased reflectivity beyond 160 km as shown in Fig. 2. We intend to do so in future work by comparing with a much denser network of daily reporting gauges from the provinces of Quebec and Ontario. In this article, we are thus essentially evaluating the skill of the four observed VPRs within 90 km as used by the  $C_1$  and  $C_2$  methods. They may be called "local" VPRs as done by Vignal et al. (1999), but in a strictly one-dimensional, that is, range-dependent way.

Although the measurements from the Mesonet can be retrieved at an hourly frequency, we have chosen for the moment to acquire the hourly totals for the previous day at only one appropriate time after midnight, compute the 24-h precipitation totals and compare them with the corresponding radar estimates. During the 'shakedown' period of last summer, these comparisons were obtained by user-interaction with the RAPID system. Clicking on the 24-h accumulation map produced at midnight, or on a shorter one from the previous day, would result in a graphic depiction of the radar-gauge comparisons. While the interactive facility has been maintained, the process of comparing daily accumulations at 0000 UTC became automated by early fall, but the resulting plots and corresponding radar-gauge (R-G) values were not archived until late March 2005. (We note here that radar-Mesonet comparisons of snowfall amounts from December to March could not be made because frozen precipitation is not reported). The interactive facility permits another comparison in which some (R-G) pairs are omitted for a variety of reasons: faulty gauge readings, R-G differences caused by strong rainfall gradients and erroneous radar estimates due to an incomplete removal of AP echoes.

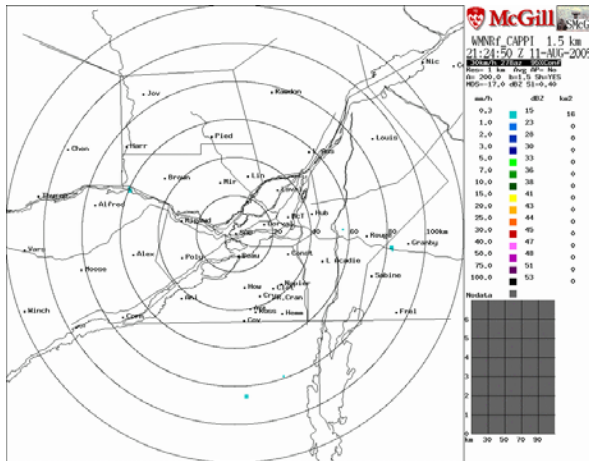


**Fig. 5:** Location of the Mesonet gauges within the McGill radar coverage. Range rings are 20 km apart to a maximum west-east range of 120 km.

The availability of archived comparisons facilitates the summary of the results and allows a quick re-analysis for different radar and/or gauge rainfall thresholds as well as for the omission of R-G pairs for similar reasons as outlined above, but which were not evident in real-time. The spring 2005 data set archived in real-time consists of 43 days of precipitation from 1 April to 24 June. About 10 R-G pairs have thus been excluded from this data set. However, we have chosen not to adjust the radar estimates for a mean field bias, because part of our goal is to assess the accuracy of real-time VPR corrected rainfall estimates, not those computed from a post facto analysis. Errors associated with fluctuations in the radar calibration,

and, especially, with the variability of the Z-R relationship are thus compounded with those due to the VPR. On the other hand, radar estimates for the major rainfall events from September to late November 2004 have been re-generated from the archived raw volume scans using the RAPID simulation facility by taking into account some known calibration variation and by adjusting for a more suitable Z-R relationship. In this effort, we have implemented a procedure outline by Lee and Zawadzki (2005a & b) that incorporates data from a disdrometer nearly collocated with the radar site. We have selected ten days, from 9 September to 28 November, all strong stratiform systems and, except for the first one (the remnants of Hurricane Francis), all characterized by relatively low bright band heights. By contrast, the spring 2005 data set includes a variety of precipitation systems; stratiform with the bright band at various heights, as well as convective and/or cellular, with some instances of evaporation and with a large range in daily rainfall amounts.

## 4. RESULTS

### a) Verification statistics

We use the well-known statistics of bias (B), mean absolute difference (AD) and root-mean-square error, (RMS), the latter two normalized by the average gauge rainfall and expressed as a percentage to verify the skill of the various methods tested for each data set. In Table 1 we also provide the cross-correlation coefficient CC and the number N of radar-gauge (R-G) comparisons. The choice of the rainfall threshold affects the resultant statistics, as well as whether it is required that such threshold be exceeded by only the gauge measurement or by either the gauge or the radar estimate. We have opted to present the results in Table 1 for a requirement of 2 mm on only the gauge in order to concentrate on significant rainfalls.

**Table 1:** Summary of the statistical scores for the two data sets obtained for all N radar-gauge pairs with  $G > 2$  mm.

| 9 September to 28 November 2004 $G_{avg}=15.7$ mm |     |      |      |      |      |
|---|-----|------|------|------|------|
|   | N   | B    | AD   | RMS  | CC   |
| $C_0$   | 209 | 1.32 | 44.7 | 95.9 | 0.87 |
| $C_1$   | 209 | 1.07 | 34.4 | 61.6 | 0.95 |
| $C_2$   | 209 | 1.05 | 25.4 | 41.2 | 0.95 |
| $C_3$   | 209 | 0.95 | 28.9 | 43.2 | 0.94 |

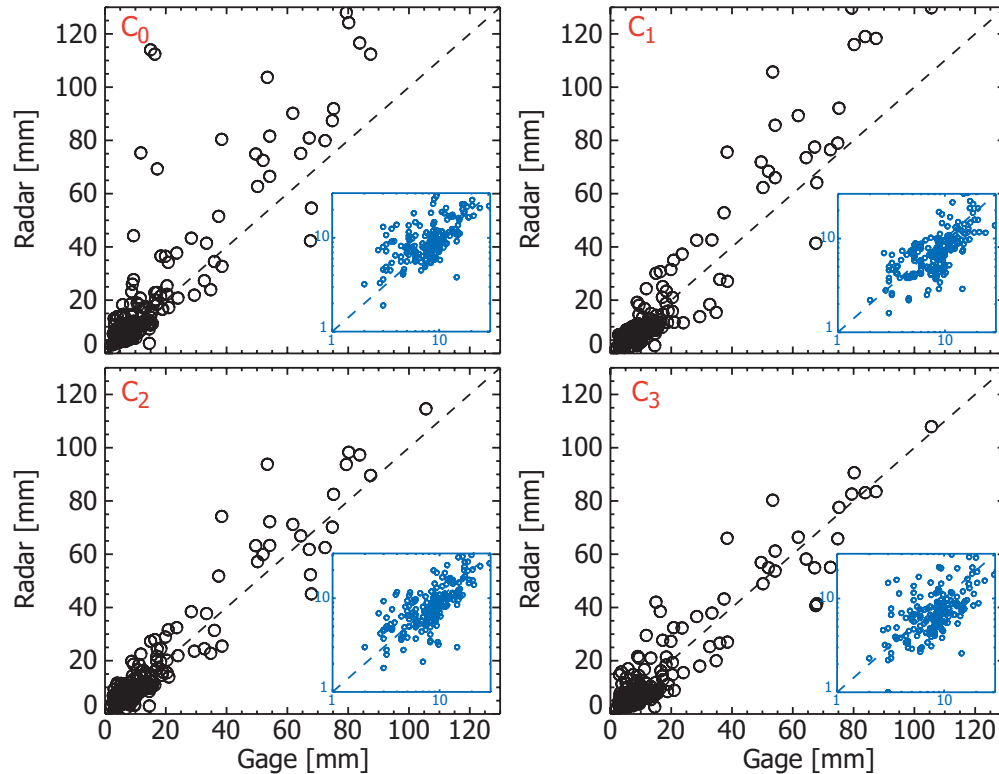
  

| 1-April to 24 June 2005 $G_{avg}=10.8$ mm |     |      |      |      |      |
|---|-----|------|------|------|------|
|   | N   | B    | AD   | RMS  | CC   |
| $C_0$                                     | 793 | 1.02 | 37.2 | 55.8 | 0.76 |
| $C_1$                                     | 793 | 0.85 | 36.0 | 53.2 | 0.79 |
| $C_2$                                     | 793 | 0.92 | 31.5 | 47.4 | 0.83 |
| $C_3$                                     | 793 | 0.80 | 37.0 | 54.1 | 0.80 |

Tests with thresholds from 0.1 to 5.0 mm yielded the expected improvement in the error statistics,

particularly with the lesser rainfalls of the spring data set, mainly due to their effect on the corresponding average rainfall. However, the relative skill of the various procedures remained essentially unaltered. Similarly, the acceptance of R-G pairs with either the radar or gauge exceeding the rainfall threshold caused a slight increase of the error scores, but again without affecting the conclusions about the relative merit of the compared methods. One distinct advantage of such a choice is that it eliminates unwanted comparisons with faulty gauges that fail to report a rainfall as well as instances of radar overestimations of light rainfalls

under conditions of evaporation for which our techniques were not designed. The radar estimate selected for the comparison is the average of the nine (1 km by 1 km) Cartesian pixels centered on the gauge location. Results are only marginally affected by selecting the centre pixel, while better scores are obviously obtained by seeking the best match in that neighborhood, the latter choice being perhaps more meaningful for convective precipitation. However, since the relative skill of the various methods is again not influenced by these different approaches, they are not presented here.



**Fig. 6:** Scatter plots of daily accumulation for the fall events for the four VPR correction methods tested. In order to better visualize the comparisons for rainfalls less than 30 mm, a logarithmic zoom has been provided.

Since the selected 10 fall events consist of strong stratiform systems, often with a low bright band, that have the most to benefit from a VPR correction, the various VPR corrections schemes reveal a greater improvement than with the spring dataset that includes all the raining days over a certain period.  $C_2$  yields the largest error reduction in both data sets; for example, RMS is reduced from 96% to 41% for the fall events and from 56% to 47% for spring 2005. The AD score is less sensitive to corrections of large overestimations, yielding smaller differences. The cross-correlation coefficient is affected by an even smaller degree and does not appear to be a suitable verification parameter.

The limited sample of the fall events with only slightly over 200 comparisons is susceptible to the

strong influence of some key days. For example, excluding the very low bright band case of 21-November, in which the VPR schemes performed very well, would drastically reduce the RMS error for  $C_0$  to 63% (from 96%). Since the score for  $C_2$  is maintained at 39%, the gap between these schemes is sharply lessened.  $C_1$  and  $C_3$  perform with some skill with the fall events but yield negligible improvement over the entire spring period. The rather disappointing result with the climatological algorithm may be due to the fact that the profiles on which it is based are computed for intense stratiform systems, a situation not typical of the 2005 data set. The difficulties discussed in section 2d associated with this method may have further reduced its effectiveness as is the accuracy with which the  $0^\circ$  C height information is provided by the model. We conclude that it should not be applied to all types of

precipitation, thus rendering its real-time application doubtful.

The scatter plots of the four comparisons for the fall events are presented in Fig. 6. On account of the wide range of daily rainfall amounts during this period, we add a logarithmic zoom view for rainfalls < 30 mm. The better performance of  $C_2$  (and of  $C_3$ ) is evident here but not in Fig 7 containing the scatter plots for the spring dataset, where even the improvement by  $C_2$  is not well depicted.

We have stated that the spring 2005 comparisons have been tabulated as computed in real-time without first correcting for the mean field bias for each day. Consequently, the bias and error scores do not reflect the true skill of the methods tested because of the influences of other sources of error. The overall bias shown on Table 1 seems to indicate that a general underestimation of the rainfall has been rendered worse by the VPR correction schemes. The cause of the underestimation is not necessarily an improper radar calibration, but could equally be an inappropriate Z-R relationship, the two sources of error being largely indistinguishable. The availability of a disdrometer in close proximity to the radar permits a verification of both its calibration status and a determination of the optimum Z-R relationship to be used on a given day Lee and Zawadzki (2005a). The case of 23 April 2005 in Fig. 8 well illustrates how an improper Z-R relationship can mask the improvement of a VPR correction scheme. The left hand plots are the real-

time comparison obtained with the climatological  $Z = 200 R^{1.5}$  relationship showing an apparent overestimation, ( $B=1.18$ ), being reduced by  $C_2$  to an underestimation, ( $B=0.83$ , while only marginally improving the RMS error from 44 to 40%. A disdrometer analysis later revealed that this day was characterized by drizzle precipitation necessitating a Z-R relationship of the order of  $Z=140R^{1.6}$ . When the comparison is repeated after regenerating the radar estimates with the updated Z-R relationship, it is revealed that the true overestimation of over 40% is properly reduced to a mere 6% while the RMS error is decreased from 59 to 36%. A similar situation has been seen for a few other days, notably on 17 June when again drizzle precipitation initially underestimated by the climatological Z-R relationship was further underestimated by the correction schemes. At other times, when an underestimation by  $C_0$  is rendered worse by all the VPR correction schemes, the need for a long, uninterrupted precipitation period for a robust disdrometer analysis prevents the reaching of a similar conclusion. Nonetheless, we can conclude that the true skill of a real-time VPR correction scheme cannot be fully realized unless the bias of the uncorrected estimates can be detected and removed in an operational environment. Attempting such a procedure in real-time, whether using disdrometric data or with a dense network of raingauges, represents an interesting challenge.

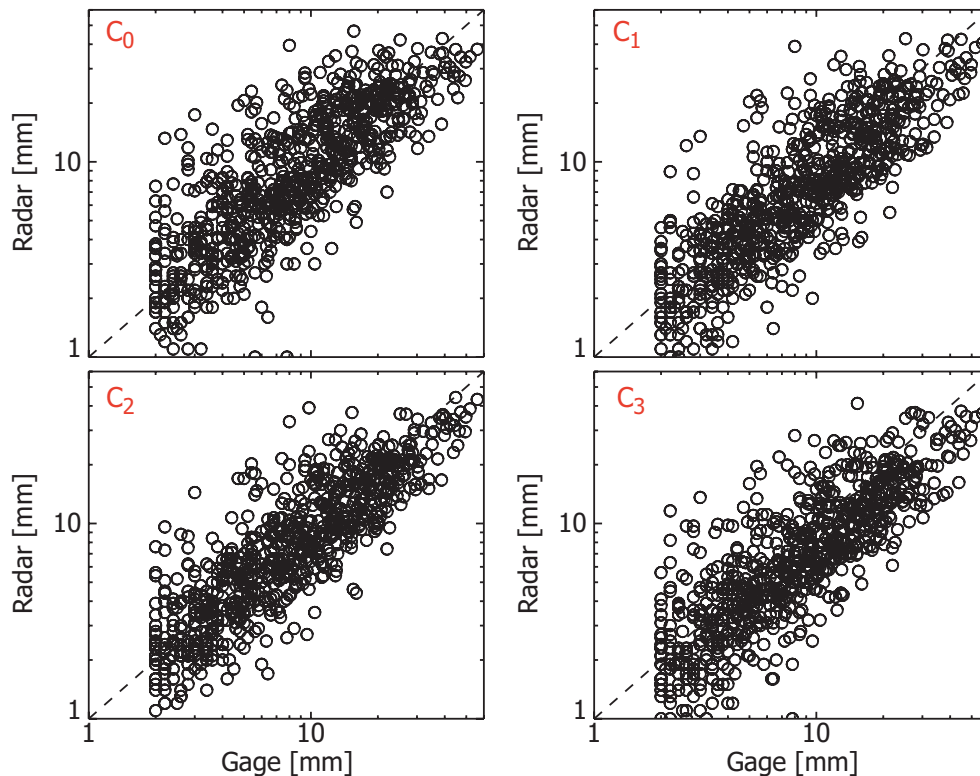
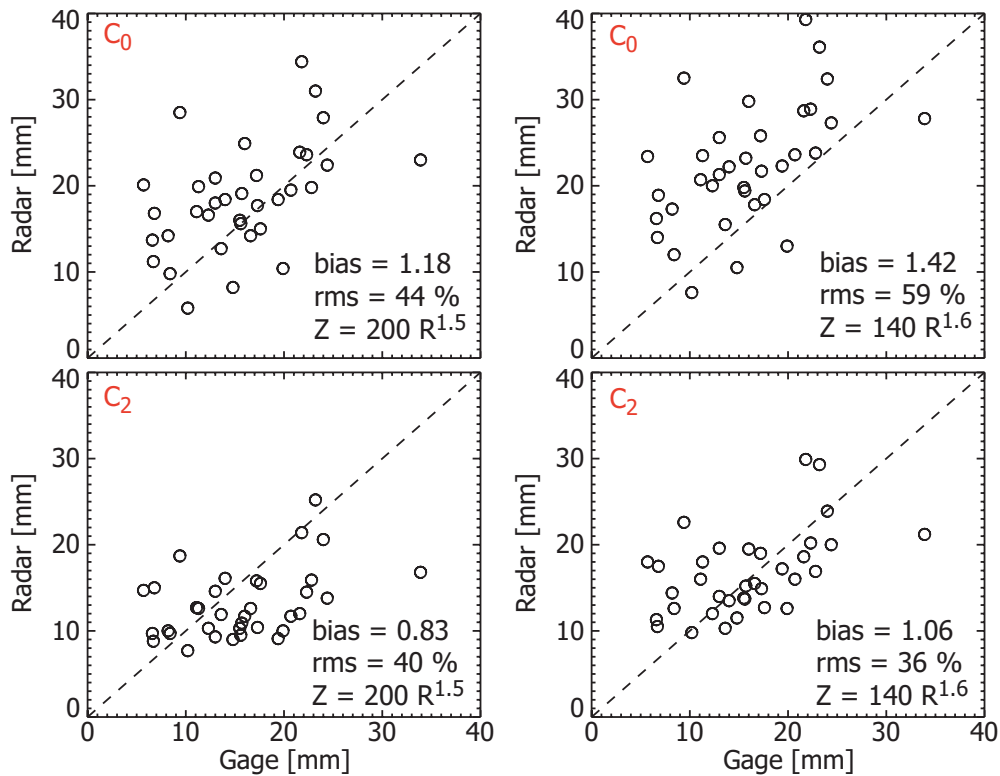


Fig. 7: Scatter plots of daily accumulation for the spring events for the four VPR correction methods tested.



**Fig. 8:** Scatter plots for the  $C_0$  and  $C_2$  comparisons on 23 April 2005 with the climatological algorithm  $Z = 200 R^{1.5}$  and with the disdrometer-derived  $Z = 140 R^{1.6}$  relationship showing how the bias from an improper Z-R can mask the true skill of a VPR correction scheme.

## 5. CONCLUSIONS

We have verified the relative skill of three VPR correction techniques for daily accumulations on a selected and on a real-time data set. The first technique ( $C_1$ ) adjusts already-derived 1-h rainfall amounts on a Cartesian map in a “one-step” procedure using the range-dependent space-time averaged VPR appropriate for that interval. The  $C_2$  technique corrects the 5-min polar reflectivity measurements categorized as stratiform precipitation according to the VPR available at the time of each of the 12 scanning cycles. It allows for a different Z-R relationship between the convective and stratiform pixels and partially takes into account evaporation, low level growth and beam blocking.  $C_3$  uses a reflectivity-dependent climatological VPR to correct the stratiform pixels. The first data set consists of 10 events during fall 2004 (9 September to 28 November) selected because they consisted exclusively of stratiform precipitation. The second data set is the series of archived comparisons made continuously in real-time for all the 43 days with precipitation from 1 April to 24 June 2005. Unlike the post facto analysis of the fall set, no adjustment for the mean field bias has been attempted with the real-time set because we wanted to duplicate an operational environment where such a procedure is still considered risky. The results on Table

1 emphasize the crucial importance of the choice of data sets, causing differences in the final assessment that are far greater than those between the various algorithms. Each of the three techniques perform well with the fall data set, particularly  $C_2$ . This is not surprising considering that the fall data set consists of events with low bright band and thus with the greatest potential for improvement. However, when the VPR algorithm was tested in a real-time environment consisting of less strong or higher bright band situations, and facing a variety of day-to-day precipitation, the improvement is substantially lower, even with  $C_2$ . RMS errors are reduced only marginally, from 56 to 47% in contrast with the 96 to 41% reduction seen with the fall events. This is because other sources of error, in particular, the variability in the Z-R relationship, are often of the same magnitude as the VPR errors. There is also the possibility that in the spring data set, unlike the fall events with extensive coverage, corrections may have been made with VPRs that were based on insufficient past data.

The results of an evaluation of any technique with selected cases should be accepted with caution if such a technique is meant for real-time operational applications. In our case, the need to pre-correct for the mean field bias using an appropriate Z-R relationship is of

primordial importance, and, to a lesser extent, the necessity to monitor the radar calibration. We hope to achieve this goal by applying emerging techniques by Lee and Zawadzki (2005a and b) that incorporate data from a disdrometer and a scanning radar. We remain aware of the limitations of disdrometric measurements at a point.

## 6. REFERENCES

- Andrieu, H., and J. D. Creutin, 1995: Identification of vertical profiles of radar reflectivity for hydrological applications using an inverse method. Part I: Formulation. *J. Appl. Meteor.*, **34**, 225-239.
- Bellon, A., and A. Kilambi, 1999: Updates to the McGill RAPID system. *29<sup>th</sup> Int. Conf. Radar Meteorology.*, Montreal, Canada, AMS, 121-124.
- Bellon, A., G. Lee and I. Zawadzki, 2005: Error statistics of VPR corrections in stratiform precipitation. *J. Appl. Meteor.*, **44**, 998-1015.
- Dinku, T., E. N. Anagnostou and M. Borga. 2002: Improving Radar-Based Estimation of Rainfall over Complex Terrain. *J. Appl. Meteor.*, **41**, 1163-1178.
- Fabry, F., G. L. Austin, and D. Tees, 1992: The accuracy of rainfall estimates by radar as a function of range. *Quart. J. Roy. Meteor. Soc.*, **118**, 435-453.
- Germann, U., and J. Joss, 2002: Mesobeta profiles to extrapolate radar precipitation measurements above the Alps to the ground level. *J. Appl. Meteor.*, **41**, 542-557.
- Greene, D. R. and R. A. Clark, 1972: Vertically Integrated Liquid water Content- A new analysis tool. *Mon. Weather Rev.*, **100**, 548-552.
- Joss, J., and A. Waldvogel, 1990: Precipitation measurement and hydrology. Pp 577-606 in *Radar in meteorology*, American Meteorological Society.
- Joss, J., and R. Lee, 1995: The application of radar-gauge comparisons to operational precipitation profile corrections. *J. Appl. Meteor.*, **34**, 2612-2630.
- Kitchen, H., 1997: Towards improved radar estimates of surface precipitation at long range. *Q. J. R. Meteorol. Soc.*, **123**, 145-163.
- Koistinen, J., 1991: Operational correction of radar rainfall errors due to the vertical reflectivity profile. Preprints, *25<sup>th</sup> Int. Conf. on Radar Meteorology*, Paris, France, Amer. Meteor. Soc., 91-94.
- Lee, G. W. and I. Zawadzki., 2005a: Variability of drop size distributions: Time scale dependence of the variability and its effects on rain estimation. *J. Appl. Meteor.*, **44**, 241-255.
- Lee, G. W. and I. Zawadzki, 2005b: Radar calibration by gage, disdrometer, and polarimetry: theoretical limit caused by the variability of drop size distribution and application to fast scanning operational radar data. *J. Hydro.* (Accepted)
- Lee, G., Y.-H. Cho, K.-E. Kim, and I. Zawadzki, 2005: Identification and removal of non-precipitation echoes using the characteristics of radar echoes. *32<sup>nd</sup> Int. Conf. Radar Meteorology.*, Albuquerque, AMS, Paper 4R.3 in this conference.
- Mittermaier, M. P., and A. J. Illingworth, 2003: Comparison of model-derived and radar-observed freezing-level heights: Implications for vertical reflectivity profile-correction schemes. *Q. J. R. Met. Soc.*, **129**, 83-95.
- Marshall, J. S., 1957: The constant-altitude presentation of radar weather patterns. *6<sup>th</sup> Conf. on Radar Meteor.*, AMS, 321-324
- Marshall, J. S., and E. H. Ballantvne, 1975: Weather Surveillance Radar. *J. Appl. Meteor.*, **14**, 1317-1338.
- Seo, D.-J., J. Breidenbach, R. Fulton, D. Miller and T. O'Bannon, 2000: Real-time adjustment of range-dependent biases in WSR-88D rainfall estimates due to nonuniform vertical profile of reflectivity. *J. of Hydrometeor.*, **1**, No. 3, 222-240.
- Smyth, T. J., and A. J. Illingworth, 1998: Radar estimates of rainfall rates at the ground in bright band and non-bright band events. *Q. J. R. Met. Soc.*, **124**, 2417-2434.
- Vignal, B., H. Andrieu, and J. D. Creutin, 1999: Identification of vertical profiles of reflectivity from volume scan radar data. *J. Appl., Meteor.*, **38**, 1214-1228.
- Vignal, B., and W. F. Krajewski, 2001: Large-scale evaluation of two methods to correct range-dependent error for WSR-88D rainfall estimates, *J. Hydrometeor.*, **2**, 490-504.
- Vignal, B., G. Galli, J. Joss, and U. Germann, 2000: Three methods to determine profiles of reflectivity from volumetric radar data to correct precipitation estimates. *J. Appl. Meteor.*, **39**, 1715-1726.